Experimental Demonstration of a Wideband Photonic Temporal Hilbert Transformer Based on a Single Fiber Bragg Grating

Ming Li, *Member, IEEE*, and Jianping Yao, *Senior Member, IEEE*

***Abstract*—A wideband photonic temporal Hilbert transformer implemented based on a single fiber Bragg grating (FBG) is experimentally demonstrated. Two FBGs with bandwidths of 50 and 100 GHz are designed and fabricated. The use of the fabricated FBGs to perform real-time temporal Hilbert transformation of a Gaussian-like optical pulse with a bandwidth of about 12 GHz is experimentally demonstrated.**

***Index Terms*—Fiber Bragg gratings (FBGs), Fourier optics and signal processing, temporal Hilbert transformer (THT), ultrafast optical signal processing.**

I. Introduction

TEMPORAL Hilbert transform (THT) is among the many important signal processing functions that is widely used in communication systems, radar, and other warfare and civil systems [1]. Compared with pure electronic implementation, photonic THT implemented in the optical domain provides a much higher speed and wider bandwidth. A photonic THT using a multitap photonic transversal system was demonstrated recently [2]. Since numerous devices such as multiple electrooptic modulators, optical delay lines, and laser sources are used in the system, the system is complicated and costly [2]. In addition, the implementation bandwidth of the photonic THT in [2] is limited to 40 GHz. To achieve an implementation bandwidth larger than 40 GHz, more taps with accurately controlled time delays are required which would again increase the implementation complicity and cost.

Recently, photonic THTs implemented based on fiber Bragg gratings (FBGs) have attracted great interest thanks to the advantageous features such as simple structure and good compatibility with other fiber-optic devices [3]–[6]. One limitation of the photonic THT reported in [2] is that the THT can only operate on the temporal intensity profile of the input waveform which is different from the photonic THTs proposed in [3]–[6] and in this letter, where the THTs can operate on the temporal complex envelope of the input waveform. A photonic THT can be implemented using a sampled FBG to form a multitap photonic transversal filter [3]. The major limitation associated with this approach is that the implement error of the THT is intimately related to the number of the sampling period, i.e., the count of taps. Therefore, for a photonic THT having a broader bandwidth, the sampling period will be smaller and the needed number of sampling period will be increased largely which would make the fabrication of the photonic THT very difficult. On the other hand, a photonic THT can also be implemented using a uniform weak-coupling FBG with a π phase shift in the FBG [4], [5]. Compared with the approach using a sampled FBG, the use of a π phase-shifted FBG is easier to implement. The main limitation of this technique is that the FBG should be weak enough to satisfy the Born approximation for the synthesis of the FBG based on space-to-frequency-to-time mapping (SFTM), making the FBG fairly weak, leading to a poor signal-to-noise ratio (SNR) at the output of the THT [7]. The SFTM method only considers one reflection during the design of an FBG, while the discrete layer peeling (DLP) method considers multiple reflections. So, the DLP method has the intrinsic advantage of higher accuracy for the design of an FBG with a high index modulation. Note that, since the index modulation of the THT designed in [4] is very weak (only about 4×10^{-4}), a processing error of about 0.3% is resulted for the design of a THT.

Very recently, we proposed to implement a photonic THT based on an FBG that was directly designed by the DLP method [6]. The significance of using the DLP method for the FBG design is that the FBG is ensured to have a strong strength, which is essential for optical signal processing with a good SNR [8], [9]. The FBG to implement the photonic THT reported in [6] was investigated numerically; no experimental demonstration was performed. In this letter, the use of an FBG for wideband photonic THT is investigated experimentally. Note that, although some experimental results have been presented in [10], detailed analyses, such as the processing error due to the fabrication tolerance and the limitations of the proposed approach, have not been addressed. Two FBGs with bandwidths of 50 and 100 GHz are designed based on the DLP method and fabricated. The use of the FBGs to perform Hilbert transform of a Gaussian-like optical pulse with a bandwidth of about 12 GHz is experimentally demonstrated.

II. Principle

Mathematically, the temporal envelope of an output optical signal $y(t)$ from a THT is given by [1]

$$y(t) = x(t) * \frac{1}{\pi t} = \mathrm{P.V.}\left[\frac{1}{\pi}\int_{-\infty}^{\infty}\frac{x(\tau)}{t-\tau}d\tau\right] \quad (1)$$

Manuscript received May 06, 2010; revised July 03, 2010; accepted August 08, 2010. Date of publication August 12, 2010; date of current version October 06, 2010. This work was supported by the Natural Sciences and Engineering Research Council of Canada (NSERC).

The authors are with the Microwave Photonics Research Laboratory, School of Information Technology and Engineering, University of Ottawa, Ottawa, ON K1N 6N5, Canada (e-mail: jpyao@site.uOttawa.ca).

Color versions of one or more of the figures in this letter are available online at http://ieeexplore.ieee.org.

Digital Object Identifier 10.1109/LPT.2010.2066964

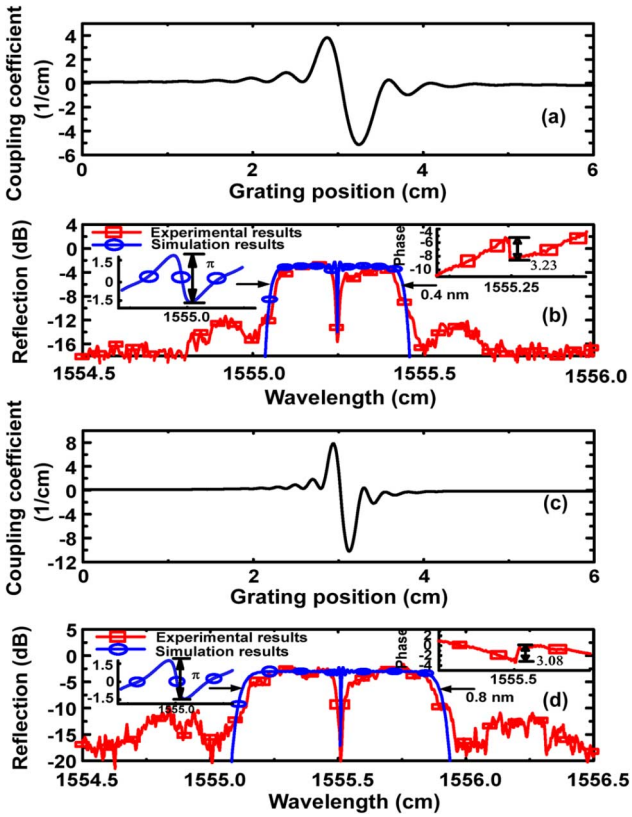

Fig. 1. Coupling coefficient profiles and reflection spectra of the designed and fabricated FBGs. (a) The coupling coefficient profile of the photonic THT with a bandwidth of 50 GHz, (b) and the corresponding reflection spectra of the designed (line+circle) and fabricated (line+square) FBGs. (c) The coupling coefficient profile of the photonic THT with a bandwidth of 100 GHz, (d) and the corresponding reflection spectra of the designed (line+circle) and fabricated (line+square) FBGs. The insets in (b) and (d) show the phase responses of the designed (line+circle) and fabricated (line+square) FBGs with a π phase shift at the notch wavelength.

where $x(t)$ is the temporal envelope of the input optical pulse, t is the time variable, $*$ denotes the convolution operator, and P.V. means principal value. By applying the Fourier transform to both sides of (1), we then have

$$Y(\omega) = X(\omega) \times [-j\mathrm{sgn}(\omega)] \tag{2}$$

where $X(\omega)$ is the Fourier transform of the input optical signal, $Y(\omega)$ is the Hilbert-transformed output optical signal, and $\mathrm{sgn}(\omega)$ is a sign function (-1 for $\omega < 0$, 0 for $\omega = 0$, and 1 for $\omega > 0$). Obviously, the transfer function of a THT in the frequency domain is $-j\mathrm{sgn}(\omega)$. To implement the photonic THT, an FBG with a frequency response of $-j\mathrm{sgn}(\omega)$ is required [6]. As can be seen, a π phase shift should be introduced to the frequency response of the FBG.

Based on the DLP method, an FBG with the desired frequency response is first designed [6]. The 3-dB bandwidth of the designed FBG is 50 GHz; the central wavelength is 1550 nm. Fig. 1(a) shows the coupling coefficient profile of the designed FBG with its phase and reflection spectra showing in Fig. 1(b). The bandwidth of the synthesized FBG is 0.4 nm (i.e., 50 GHz). A π phase shift is realized at the central wavelength, as shown in the inset (line+circle) of Fig. 1(b). Based on the same design strategy, a photonic THT with a bandwidth of 100 GHz (i.e., 0.8 nm) is also successfully designed with the simulation

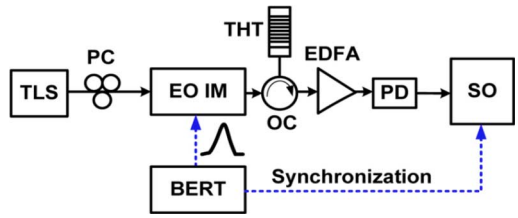

Fig. 2. Experimental setup. TLS: tunable laser source; PC: polarization controller; EO IM: electrooptic intensity modulator; THT: temporal Hilbert transformer; OC: optical circulator; EDFA: erbium-doped fiber amplifier; PD: photodetector; SO: sampling oscilloscope; BERT: bit-error-rate tester.

results showing in Fig. 1(c) and (d). Note that the coupling coefficient profiles shown in Fig. 1(a) and (c) are very similar to those designed based on the SFTM method, but the reflectivities of the FBGs based on the SFTM method are smaller than 50% to ensure an acceptable processing accuracy. Therefore, a THT could be designed using the SFTM method, but with a reflectivity usually smaller than 50%.

III. Experiment

Based on the calculated coupling coefficient profiles, as shown in Fig. 1(a) and (c), the two FBGs are then fabricated via UV illumination by a frequency-doubled argon-ion laser operating at 244 nm and a uniform phase mask. The apodization is implemented by dephasing the subsequent exposures while the UV beam is scanning the mask similar to the technique in [11]. Fig. 1(b) shows the reflection and phase spectra of the fabricated 50-GHz photonic THT measured by using an optical vector analyzer (OVA). A good agreement between the experimental and numerical results is achieved. A phase shift of 3.23 which is very close to π is experimentally realized at the notch wavelength, as shown in the inset (line+square) of Fig. 1(b). The measured notch depth is about 14 dB. For the 100-GHz photonic THT, the desired reflection and phase responses are experimentally obtained, as shown in Fig. 1(d). A phase shift of 3.08 is realized, and the notch depth is about 17 dB.

One may note that the central wavelengths of the designed FBGs are both 1555.00 nm, while the central wavelengths of the fabricated photonic THTs in Fig. 1(b) and (d) are 1555.25 and 1555.50 nm, respectively. The discrepancy in wavelength is caused by the residual strain during the FBG writing process. For the sake of an easy comparison, the central wavelengths of the theoretically obtained reflection spectra are shifted to the measured wavelengths. In addition, for an FBG having a spectral response with a finite width, the FBG should have a physical length that is infinite, which is not possible for practical implementation. Therefore, in the design the lengths of the FBGs are truncated, which will lead to sidelobes in the spectral response, as can be seen from Fig. 1(b) and (d).

To verify that the fabricated FBGs can be used to implement real-time temporal Hilbert transform, an experiment is then carried out based on an experimental setup shown in Fig. 2. A CW light wave from a tunable laser source (TLS) is directed to an intensity modulator (IM). An electrical pulse train with a bit rate of 13.5 Gb/s from a bit-error-rate tester (BERT, Agilent 4901B), as shown in Fig. 3(a), is applied to modulate the optical carrier at the IM. The pulse from the BERT has a shape close to a Gaussian with a full-width at half-maximum (FWHM) of about 63 ps. Since the input pulse is not a standard Gaussian pulse,

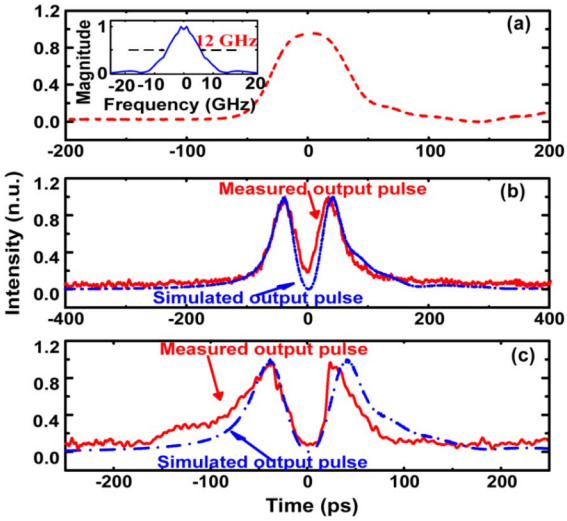

Fig. 3. Experimental results. (a) The input pulse from the BERT, the inset shows the frequency spectrum of the input pulse, (b) the simulated (dashed–dotted line) and measured (solid line) output pulses from the photonic THT with a bandwidth of 50 GHz, (c) and the simulated (dashed–dotted line) and measured (solid line) output pulses from the photonic THT with a bandwidth of 100 GHz.

the bandwidth of the input pulse at the FWHM in the frequency domain is calculated to be about 12 GHz, as shown in the inset of Fig. 3(a). The optical signal is then sent to the FBG through an optical circulator (OC). The Hilbert transformed pulse is amplified by an erbium-doped fiber amplifier (EDFA) and then detected by a high-speed photodetector (PD) with its waveform observed by a high-speed sampling oscilloscope [(SO) Agilent 86116A].

Fig. 3(b) shows the measured output pulse from the photonic THT with a bandwidth of 50 GHz. A simulated pulse is also shown in Fig. 3(b). As can be seen, the simulated and experimental results agree well. The root mean square (rms) error is calculated to be about 7.8%. The photonic THT with a bandwidth of 100 GHz is also evaluated. The simulated and experimental results are shown in Fig. 3(c). Again, a good agreement is reached. The rms error is about 15.1%.

Processing error as a function of the input pulse bandwidth is estimated based on the measured magnitude and phase responses of the fabricated THTs. To implement this evaluation, the amplitude and phase responses of the fabricated 50- and 100-GHz THTs are first measured using the OVA, and then the output pulse for an input Gaussian pulse with different bandwidth is calculated. The processing error is then obtained by calculating the rms error for the Gaussian pulse with a bandwidth from 0 to 200 GHz, as shown in Fig. 4(a). It can be seen that there exists an optimal operation bandwidth where the rms error is minimized for the THT. In addition, it is obvious that the processing error is significantly increased when the bandwidth of the input pulse is closed to zero, which is caused by the notch at the central wavelength that should be eliminated for an ideal Hilbert transformer. However, the notch will be always formed when a π phase shift is introduced into the FBG-based THT. So, the processing error of the proposed THT will be intrinsic large for an input signal with a narrow bandwidth.

In general, the phase shift in a fabricated THT cannot be exactly controlled to be π at the central wavelength due to the fabrication error. To evaluate the influence of the phase shift deviation on the THT performance, the processing error of the THT with different phase shift deviations is calculated, as shown in Fig. 4(b). It can be seen that the rms error is increasing almost linearly with the increase of the phase shift deviation.

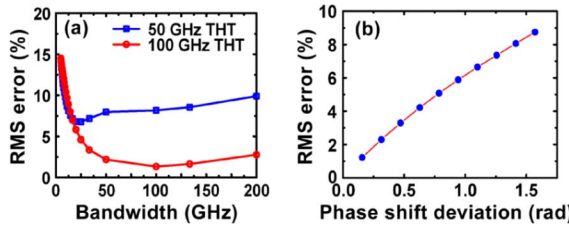

Fig. 4. (a) Estimated processing error as a function of the input pulse bandwidth for the fabricated 50 GHz (line+square) and 100 GHz (line+circle) THTs. RMS: root mean square. (b) Simulation results of the processing error caused by the phase shift deviation.

IV. Conclusion

The implementation of a wideband photonic THT based on a single FBG was experimentally demonstrated. Two FBGs with bandwidths of 50 and 100 GHz were designed and fabricated. The use of the fabricated FBGs to perform temporal Hilbert transform of a Gaussian-like optical pulse with a bandwidth of about 12 GHz was demonstrated. Processing error as a function of the input pulse bandwidth was estimated based on the measured magnitude and phase responses of the fabricated FBGs.

References

[1] S. L. Hahn, "Hilbert transforms," in *The Transforms and Applications Handbook*, A. D. Poularikas, Ed., 2nd ed. Boca Raton, FL: CRC Press, 2000, ch. 7.

[2] H. Emami, N. Sarkhosh, L. A. Bui, and A. Mitchell, "Wideband RF photonic in-phase and quadrature-phase generation," *Opt. Lett.*, vol. 33, no. 2, pp. 98–100, Jan. 2008.

[3] M. Hanawa, K. Nakamura, K. Takano, and K. Nakagawa, "All-optical Hilbert transformer for optical single-side-band modulation by using sampled fiber Bragg grating based optical transversal filter," in *ECOC 2007 Conf.*, Berlin, Germany, 2009, Paper 4.1.3.

[4] M. H. Asghari and J. Azaña, "All-optical Hilbert transformer based on a single phase-shifted fiber Bragg grating: Design and analysis," *Opt. Lett.*, vol. 34, no. 3, pp. 334–336, Feb. 2009.

[5] C. Cuadrado-Laborde, "Proposal and design of a photonic in-fiber fractional Hilbert transformer," *IEEE Photon. Technol. Lett.*, vol. 22, no. 1, pp. 33–35, Jan. 1, 2010.

[6] M. Li and J. P. Yao, "All-fiber temporal photonic fractional Hilbert transformer based on a directly designed fiber Bragg grating," *Opt. Lett.*, vol. 35, no. 2, pp. 223–225, Jan. 2010.

[7] J. Azaña and L. R. Chen, "Synthesis of temporal optical waveforms by fiber Bragg gratings: A new approach based on space-to-frequency-to-time mapping," *J. Opt. Soc. Amer. B*, vol. 19, no. 11, pp. 2758–2769, Nov. 2002.

[8] R. Feced, M. N. Zervas, and M. A. Muriel, "An efficient inverse scattering algorithm for the design of nonuniform fiber Bragg gratings," *IEEE J. Quantum. Electron.*, vol. 35, no. 8, pp. 1105–1115, Aug. 1999.

[9] J. Skaar, L. Wang, and T. Erdogen, "On the synthesis of fiber Bragg grating by layer peeling," *IEEE J. Quantum. Electron.*, vol. 37, no. 2, pp. 165–173, Feb. 2001.

[10] M. Li and J. P. Yao, "Fiber Bragg gratings for wideband temporal Hilbert transform," in *BGPP 2010 Conf.*, Karlsruhe, Germany, 2010, Paper BTuA3.

[11] M. J. Cole, W. H. Loh, R. I. Laming, M. N. Zervas, and S. Barcelos, "Moving fibre/phase mask-scanning beam technique for enhanced flexibility in producing fibre gratings with uniform phase mask," *Electron. Lett.*, vol. 31, no. 17, pp. 1488–1489, Aug. 1995.